IOP Conf. Series: Materials Science and Engineering **333** (2018) 012006 doi:10.1088/1757-899X/333/1/012006

X-RAY Diffraction and Fourier Transform Infrared Study of Ca-Mg-Al Hydrotalcite from Artificial Brine Water with Synthesis Hydrothermal Treatments

Heriyanto[1], E Heraldy[2,3] and K D Nugrahaningtyas[2,3]
[1)] Department of Chemistry, Master Program Graduate School, Sebelas Maret University
[2)] Department of Chemistry, Faculty of Mathematics and Natural Sciences, Sebelas Maret University
[3)] Solid State Chemistry & Catalysis Research Group, Sebelas Maret University
Jl. Ir. A. Sutami 36A, Kentingan, Surakarta 57126, Indonesia

E-mail: eheraldy@mipa.uns.ac.id

Abstract. Synthesis of various hydrothermal treatments for synthesis Ca-Mg-Al hydrotalcite from artificial brine water had been performed. The hydrothermal treatment has four variations with a temperature at 180 ºC into Teflon lined stainless steel for 18 hours. The XRD result of the synthesis materials after various hydrothermal treatments has hydrotalcite phase and $CaCO_3$. Therefore a preparation method might not discover a mixture of Ca and Al cations uniformly, and then a number of Ca cation agglomerated and enabled evidence that the radius of Ca^{2+} was larger than Mg^{2+}. Le Bail refinement of the value of reliability index parameter especially X^2 values has concern limitation value of reliability index. Lattice parameter a and c have a value of around 22 and 3 Å, respectively. Ca-Mg-Al hydrotalcite possesses crystallite size lower than Mg-Al hydrotalcite commercial. Infrared spectra has found hydroxyl band at region 3474.91 and 3072.74 cm^{-1}, carbonate band at region 1365.66; 1491.04; 857.40; and 685.72 cm^{-1}, and metal band at region 447.50; 553.59; 772.52 cm^{-1}; and 975.06 cm^{-1}.

1. Introduction

Hydrotalcite, layered double hydroxide, is material unique and interested in latest years due to their potential application in several fields as adsorbent [1], catalyst [2], ion exchange [1], pharmaceutical [3] and photocatalysis [4]. Structurally, hydrotalcite can explain as containing brucite $Mg(OH)_2$ like layers [5], where each Mg^{2+} cation is octahedral side share edge to form infinite sheets. According to [6], in the hydrotalcite, substitution isomorphous of Mg^{2+}/Al^{3+} is in the octahedral site of the hydroxide sheet cause a net positive charge, which is to be neutralized by anionic species in the interlayer. Hydrotalcite can be stated with $[M^{2+}_{1-x}M^{3+}_{x}(OH)_2]^{x+}(A^{n-})_{x/n}.yH_2O$ [7], where M^{2+} is a divalent cation, M^{3+} is a trivalent metal cation, and A^{n-} is the replaceable anion (usually carbonate, nitrate or chloride) and $0.2 < x < 0.33$; y is the amount of interlayer H_2O.

In the previous study, synthesis hydrotalcite from brine water with co-precipitation method especially Ca-Mg-Al hydrotalcite has another hydrotalcite phase such as $Al(OH)_3$, $Mg(OH)_2$, $Ca(OH)_2$ and $CaCO_3$ [8]. Rives (2001) reported that the parameter of an experiment may be affect the hydrotalcite crystallized, such as pH, concentration metallic salts, an alkaline solution, the flow rate of reactants, temperature in the reactor, and aging time of the precipitate. In many cases, an optimization condition

to make improvement contain hydrotalcite phase by hydrothermal treatment is in the presence of water vapor at high temperature [10]. Synthesis with various hydrothermal treatment has been studied by Hickey et al. (2000), which is used mother liquor and washed slurry hydrotalcite. For temperature hydrothermal treatment has been reported by Kovanda et al. (2005) and Sharma et al. (2007). The hydrothermal treatment for aging time has been reported Oh et al. (2002) and Sharma et al. (2007).

The objective of the current work is to study the impact of various hydrothermal treatments from artificial brine water. The synthetic hydrotalcite with Ca-Mg/Al molar ratio of 2 was synthesis under hydrothermal conditions at various treatment washed and centrifuged. An influence of hydrothermal treatment was assessed by powder X-ray diffraction (XRD) and Fourier transform infrared (FTIR).

2. Experimental

2.1 Materials

Magnesium chloride ($MgCl_2.2H_2O$); calcium chloride ($CaCl_2.2H_2O$); sodium carbonate (Na_2CO_3); aluminum chloride ($AlCl_3.6H_2O$); aquadest was used for the synthesis of Ca-Mg-Al hydrotalcite in p.a. grade from Merck, Germany or equivalent and without further treatment.

2.2 Preparation of Ca-Mg-Al hydrotalcite

Ca-Mg-Al hydrotalcite compounds with the molar ratio (Ca+Mg)/Al is 2 was prepared by co-precipitation method [14]. Artificial brine water contained a magnesium and calcium source, added $AlCl_3.6H_2O$ solution and the alkaline solution Na_2CO_3 0.1 M until pH was ≈ 10. The suspension was stirred for 1 h at 65 ºC. The slurry was divided into three portions to undergo different hydrothermal treatment. One portion (called A sample) was hydrothermal treatment at 180 ºC into Teflon lined stainless steel for 18 h [6], and then the sample was washed with aquadest until free ion Cl^- ($AgNO_3$ test). The other portion (called B sample) was washed with aquadest until free ion Cl^- and then hydrothermal treatment at 180 ºC for 18 h [12]. The last portion (called C sample) was centrifuged at 2000 rpm for 15 min, and then the slurry was divided into two portions (called C1 and C2 sample). A sample of C1 was hydrothermal treatment like as A sample method, and a sample of C2 was hydrothermal treatment like as B sample method. After all hydrothermal treatment, the slurry was separated by centrifugation at 2000 rpm for 15 min and then dried overnight at 105 ºC for the subsequent characterizations.

2.3 Characterization

The samples were recorded by a Bruker D8 Advance X-ray diffractometer using monochromatized Cu-Kα radiation. The samples were measured in the diffraction angle range 2θ from 10° to 70° with steps of 0.02°. A Jade software package (Material Data, Inc.) was used to analyze the data, identification of the existing crystalline phase being approached standard JCPDS diffraction data files. Data manipulation and interpretation were performed using OriginPro 8.0 software. The XRD pattern was analyzed by Le Bail refinement method using RIETICA program [15]. Peak profiles were modeled using a pseudo-Voigt peak shape. Experimental parameters refined were the instrument zero, scale factor, the lattice parameters and the peak shape parameters u, v, w, γ_0 and γ_1 [16]. Each refinement was conducted at 30 cycles [17].

The IR spectrum of samples was recorded at room temperature with a Fourier transform infrared (FTIR) spectroscopy Shimadzu IR-Prestige21. FTIR spectra measurements were conducted to identify the functional groups contained in the hydrotalcite crystal. Sample were contained in a KBr pellet in the range 4000-400 cm^{-1}, typically, 45 scans were performed at a resolution of 2 cm^{-1}. Data manipulation, such as baseline adjustment and fitting multi peak interpretation, was performed using OriginPro 8.0 software.

3. Result and Discussion

3.1 XRD

The XRD patterns of the synthesis materials after various hydrothermal treatments are very similar (Figure 1). The sharp and symmetric basal reflection of the 003 and 006 planes at *2θ* value 11-23º and broad, asymmetric reflections at higher *2θ* value 34-65º were observed in XRD patterns. The hydrotalcite phase (JCPDS #890460) was identified as the main crystallite phase and $CaCO_3$ (JCPDS #712396) as the secondary crystallite phase. Hydrotalcite has diffraction specific identify at *2θ* value 11,5º (d_{003}); 23,45º (d_{006}) and 34,57º (d_{009}), although *2θ* value 61,9º (d_{110}) was detected diffraction specific for anion interlayer CO_3^{2-} [1]. Gao et al. (2010) reported crystal of $CaCO_3$ can be formed because a preparation method might not discover a mixture of Ca and Al cations uniformly, then a number of Ca cation agglomerated. Another explained from the evidence that the radius of Ca^{2+} was larger than Mg^{2+} [18]. After Mg^{2+} in layers was partially replaced with Ca^{2+}, the interaction between interlayer anions and cations in layers was decreased, causing that the interaction between anion in interlayer and Ca^{2+} in layers is weaker than between anions in interlayer and Mg^{2+} in layers [9].

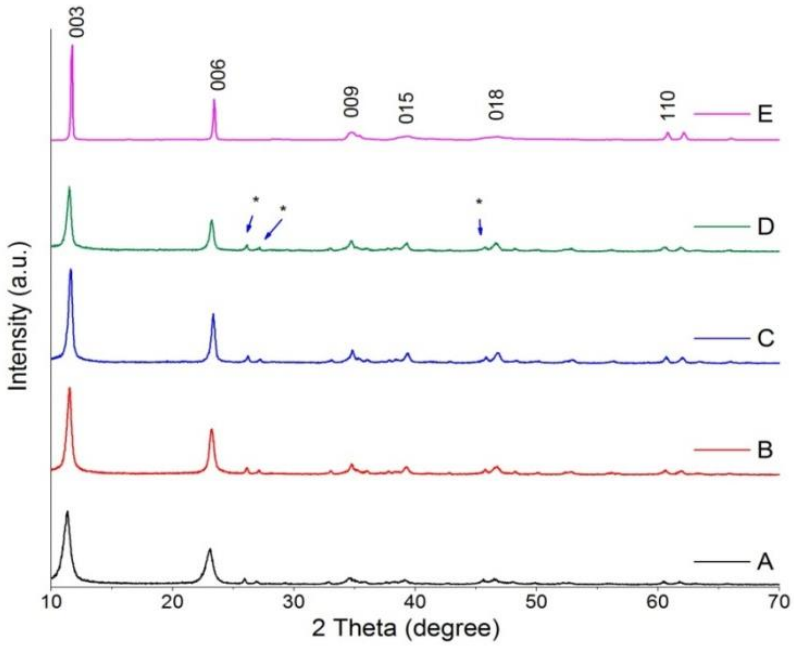

Figure 1. Diffractogram XRD Ca-Mg-Al hydrotalcite with variation treatment hydrothermal (A) sample A, (B) sample B, (C) sample C1, (D) sample C2 and Mg-Al hydrotalcite commercial (E). * = $CaCO_3$.

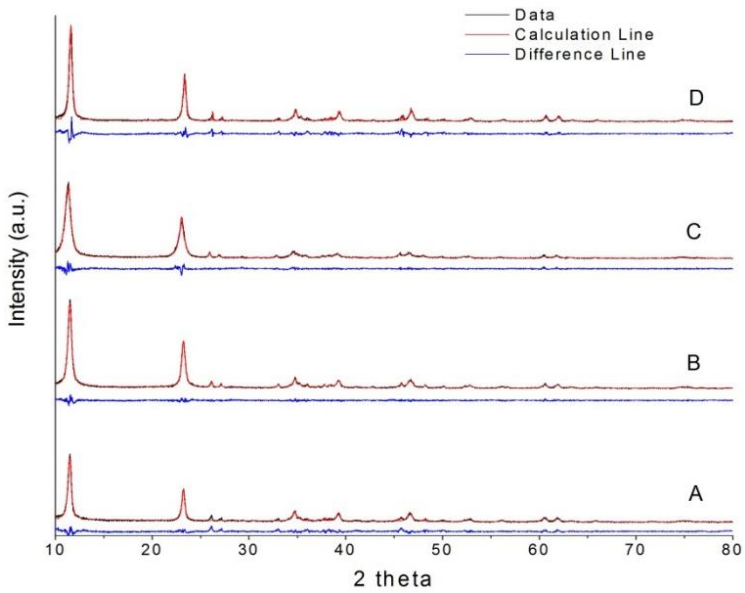

Figure 2. Observed (black), calculated (red) and difference (blue) curves of the Le Bail refine patterns of Ca-Mg-Al hydrotalcite sample that were produced hydrothermal treatment (A) sample A, (B) sample B, (C) sample C1 and (D) sample C2.

The Le Bail refinement results were shown in Figure 2. It could be seen that there was peak corresponding to the calculation results. There was peaks similarity both sample and JCPDS standard, but *Rp* and *Rwp* value result is the difference between Ca-Mg-Al hydrotalcite and standard at 2θ 11º and 23º. It is implied on the value of reliability index parameters i.e. *Rp*, *Rwp*, *Rexp*, and X^2. The limitation of value of reliability index parameters for *Rp* and *Rwp* value are 8.0 [19], while X^2 value is 4.0 [20,21]. In Table 1, all samples Ca-Mg-Al hydrotalcite has low reliability index in *Rp* and *Rwp* value, but X^2 value has concern by value of reliability index parameter.

Table 1. Le Bail reliability factor of sample Ca-Mg-Al hydrotalcite.

Sample	Le Bail reliable factors			
	Rp	*Rwp*	*Rexp*	X^2
A	10.88	14.57	11.89	1.501
B	9.16	12.74	11.03	1.333
C	10.48	14.26	11.15	1.634
D	9.82	13.35	11.16	1.433

Another sense observed was a shift toward lower and higher 2θ values of the reflections. According to the Bragg's law:

$$n\lambda = 2d\ sin\theta \quad (1)$$

where n is 1, λ is wavenumber Cu Kα, 1,54063 Å, d is basal spacing (reflectance) and θ is Bragg angle [7,9]. In the first time, hydrotalcite has a brucite-like $Mg(OH)_2$ network, and then Al^{3+} isomorphous substitution Mg^{2+} in octahedral site. In a case, three element metals like as Mg^{2+}, Al^{3+} and Ca^{2+} in hydrotalcite-like which is Ca^{2+} ions can be replaced Mg^{2+} ion in octahedral site, caused by ionic radius of Ca^{2+} (0,98 Å) was larger than that of Mg^{2+}(0,65 Å) and Al^{3+} (0,50 Å) [7]. Consequently, basal reflectance of d_{003} has become large than Mg-Al hydrotalcite commercial. In Figure 3, sample A has higher basal reflection (7.7968 Å) than Mg-Al hydrotalcite commercial (7.5632 Å). Millange et al. (2000a) reported Ca-Al hydrotalcite (hydrocalumite) has basal reflectance d_{002} at 8.7 Å. Lv et al. (2012) reported that the crystal structure of hydrotalcite could be partly damaged with the increase of amount Ca^{2+} ion to replaced Mg^{2+} in octahedral site. This clarifies calculate Le Bail refinement has higher than limitation of value of reliability index parameters.

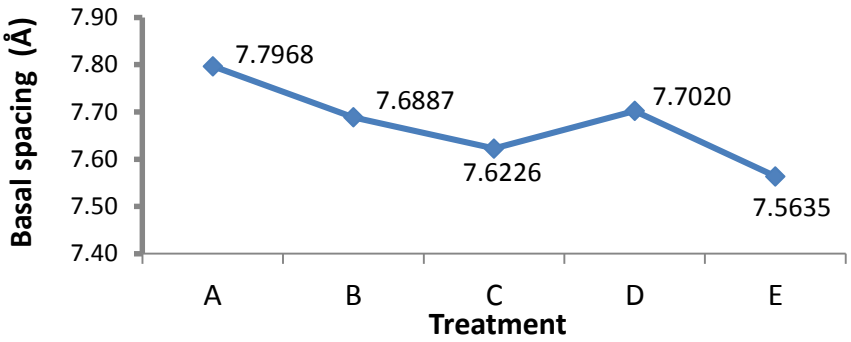

Figure 3. Basal reflection 003 Ca-Mg-Al hydrotalcite with variation treatment hydrothermal (A) sample A, (B) sample B, (C) sample C1, (D) sample C2 and (E) Mg-Al hydrotalcite commercial.

The lattice parameters *c* and *a* were determined from the basal reflectance positions of d_{003}; d_{006}; d_{009} and d_{110}, with formula $c = 3d_{003}$ and $a = 2d_{110}$ [7,10]. The *c* parameter provides data on the character, charge and size of the anion placed between the brucite-like layers. In the same way, parameter *a* can be investigated by a simple way of analyzing the isomorphic substitution of Mg^{2+} by the Al^{3+} cations. [10]. The increase in lattice parameter *c* from 22.6896 Å (sample Mg-Al commercial) to 23.3889 Å (sample C1), and each hydroxide layer increases by in 0.6993 Å thickness layer brucite-like. The increase in lattice parameter *c* (Table 2) is caused by the decrease in the electrostatic attraction between the positive brucite-like sheets and the interlayer, with modification of the OH- - -O bond strength [7]. For lattice parameter *a* has the value of around 3 Å. This is good conformity that informed in the literature [8,24]. The replacement of magnesium with aluminum or calcium leads to increase in lattice parameter *a* from 3.0446 Å (Mg-Al hydrotalcite commercial sample) to 3.5078 Å (C1 sample), reflecting the evidence that the ionic radii of Mg^{2+}, Ca^{2+} and Al^{3+} are 0.66, 0.9 and 0.56 Å, respectively [25].

The crystallite size of Ca-Mg-Al hydrotalcite was computed from the main reflection (11°) using the Scherer formula [26]:

$$\varepsilon = \frac{K\,x\,\lambda}{\beta\,x\sin\theta} \qquad (2)$$

Where ε is the crystallite size (nm); *K* is the shape factor (0.89); λ is the wavelength of the Cu Kα radiation (0.1540 nm), β is the full width at half maximum (FWHM) and θ is the Bragg diffraction angle. Mg-Al hydrotalcite commercial has crystallite size wider than sample hydrothermal treatment. Which is Mg-Al hydrotalcite commercial more crystalline in XRD patterns. In Figure 1, that shown peak in d_{003} and d_{110} has wider than Mg-Al hydrotalcite commercial, so FWHM Mg-Al hydrotalcite commercial is very low than other.

Table 2. Crystallite size Debye-Scherer and lattice parameter (a and c).

Sample	Crystallite size (nm)		Lattice parameter (Å)	
	003	110	a	c
A	2.5995	10.9154	3.0611	23.1779
B	3.6290	6.0817	3.0555	23.0971
C1	3.8499	7.0155	3.0500	22.9673
C2	4.1107	4.7634	3.0573	23.1161
Mg-Al Commercial	8.1507	5.8883	3.0446	22.6896

3.2 FTIR

The FTIR spectra for sample synthesis at hydrothermal treatment are shown in Figure 4. The region between 2600-4000 cm^{-1}, also known as the hydroxyl stretching region was characterized by broad bands at 3474.91 and 3072.74 cm^{-1}. The 3474.91 cm^{-1} band is attributed to the H-bonded interlayer H_2O surrounding the interlayer region and the metal-OH stretching mode. In this one, band cannot

distinguish between the various metal (Mg, Ca and Al) bonded to the hydroxyl groups in the infrared spectrum. The 3072.74 cm^{-1} band is in general figure out as the CO_3-H_2O bridging mode [27]. The broad band region at 1635,71 cm^{-1} was attributed the –OH deformation mode of the H_2O molecules in interlayer hydrotalcite [28]. The sharper band region at 1365.66 cm^{-1} is ascribed to the stretching mode of antisymmetric of the carbonate species existing in the interlayer, and the band region 1491.04 cm^{-1} was observed for the free CO_3^{2-} ion in the interlayer region [11].

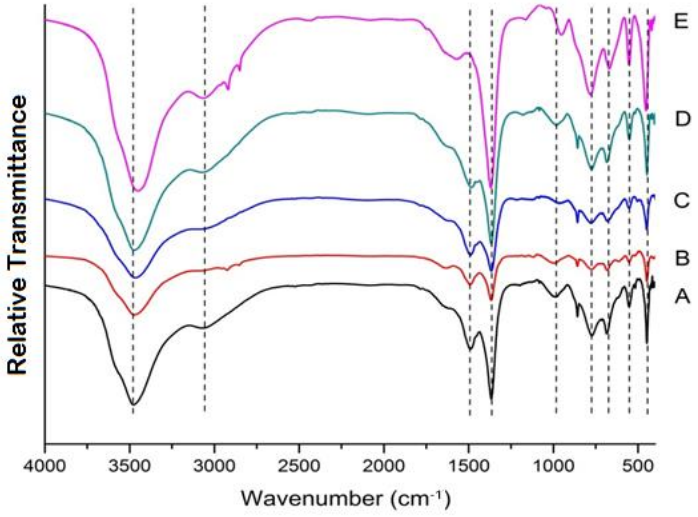

Figure 4. FTIR with variation treatment hydrothermal variation treatment (A) sample A, (B) sample B, (C) sample C1, (D) sample C2 and Mg-Al hydrotalcite commercial (E).

In Figure 4 the band region around 1400 cm^{-1} shown at Mg-Al hydrotalcite commercial has not peak of free carbonate ion. Which is due to the carbonate ion in the interlayer has bonded hydroxyl (HO-M) in layer brucite-like. The band at 685.72 and 857.40 cm^{-1} are characteristic of vibration carbonate symmetric stretching mode [29]. The band region around at 1000-400 cm^{-1} ascribed specific bonding metal (M-O) such as Mg-O, Ca-O and Al-O vibrational modes in the brucite-type layer. The band at 447.50 cm^{-1} is assigned to M^{2+}-O and band at 772.52 cm^{-1} is ascribed vibration M^{2+}-O deformation mode. Kagunya et al. (1998) reported for Ca-O and Mg-O in infrared assignments show that hydrotalcite translation modes are significantly higher frequencies than those of Mg-O. This investigation is reliable with a shorter O–H bond in hydrotalcite than in Mg-O as a result of the increased electrostatic attraction within a hydrotalcite cationic lattice due to the existing of Al cations in site of some of the Mg cations. The band Al-O is assigned to the band at 553.59 cm^{-1} and band at 975.06 cm^{-1} as vibration Al-O deformation mode [28].

4. Conclusion

In this work, Ca-Mg-Al hydrotalcite synthesized with various hydrothermal treatments was successfully prepared. Hence, artificial brine water has contained magnesium and calcium, which is can be a source of hydrotalcite synthesis. The result from this study confirmed that various hydrothermal treatment found hydrotalcite and $CaCO_3$ phase in XRD patterns. Le Bail refinement of the value of reliability index parameter especially X^2 values has concern limitation value of reliability index. A basal reflection, d, has shifted to become higher than basal reflection Mg-Al hydrotalcite commercial (7.5632 Å). The increase in lattice parameter *c* and *a* improved thickness layers brucite-like. The crystallite size has higher than Mg-Al hydrotalcite commercial. Infrared spectra have found hydroxyl band at region 3474.91 and 3072.74 cm^{-1}, carbonate band at region 1365.66; 1491.04; 857.40; and 685.72 cm^{-1}, and metal band at region 447.50; 553.59; 772.52; and 975.06 cm^{-1}.

Reference

[1] Heraldy E, Santosa S J, Triyono and Wijaya K 2015 *Indones. J. Chem.* **15** 234–41
[2] Gao L, Teng G, Xiao G and Wei R 2010 *Biomass Bioenergy* **34** 1283–8
[3] Heraldy E, Nurcahyo I F and Ainurofiq A 2012 *Prosiding InSINas 2012* pp 37–44
[4] Sarkarat M, Komarneni S, Rezvani Z, Wu X, Yin S and Yan Z 2013 *Appl. Clay Sci.* **80**–**81** 390–7
[5] Millange F, Walton R I and O'Hare D 2000 *J. Mater. Chem.* **10** 1713–20
[6] Kovanda F, Koloušek D, Cílová Z and Hulínský V 2005 *Appl. Clay Sci.* **28** 101–9
[7] Cavani F, Trifirò F and Vaccari A 1991 *Catal. Today* **11** 173–301
[8] Heraldy E, Nugrahaningtyas K D and Heriyanto 2017 *IOP Conf. Series: Materials Science and Engineering* vol 176
[9] Rives V 2001 *Layered Double Hydroxides Present and Future* (New York: Nova Science Publishers, Inc.)
[10] Sánchez-cantú M, Pérez-díaz L M, Rubio-rosas E, Abril-sandoval V H, Merino-aguirre J G, Reyes-cruz F M and Orea L 2014 *Chem. Pap.* **68** 638–49
[11] Hickey L, Kloprogge J T and Frost R L 2000 *J. Mater. Sci.* **35** 4347–55
[12] Sharma S K, Kushwaha P K, Srivastava V K, Bhatt S D and Jasra R V 2007 *Ind. Eng. Chem. Res.* **3** 4856–65
[13] Oh J M, Hwang S H and Choy J H 2002 *Solid State Ionics* **151** 285–91
[14] Heraldy E, Prasasti D, Wijaya K, Santosa S J and Triyono 2010 Studi Pendahuluan Pemanfaatan Limbah Desalinasi Untuk Pembuatan Mg/Al Hydrotalcite-Like *J. Bumi Lestari* **12** 16–23
[15] Sanches E A, Carolino A D S, Santos A L Dos, Fernandes E G R, Triches D M and Mascarenhas Y P 2015 *Adv. Mater. Sci. Eng.* **2015**
[16] Peterson V K 2005 *Powder Diffr.* **20** 14–7
[17] Heraldy E, Rahmawati F, Heriyanto and Putra D P 2017 *J. Environ. Chem. Eng* **5** ***1666-1675***
[18] Zhang M L, Gao Y and Li L F 2011 *Adv. Mater. Res.* **287**–**290** 569–72
[19] Fei L, Yanhuai L, Zhongxiao S, Kewei X, Zhi Z and Hong C 2015 *Rare Met. Mater. Eng.* **44** 2716–20
[20] Lu X, Shih K, Li X, Liu G, Zeng E Y and Wang F 2016 *Water Res.* **90** 9–14
[21] Yan H and Shih K 2016 *Water Res.* **95** 310–8
[22] Millange F, Walton R, Lei L and O'Hare D 2000 *Chem. Mater.* 1990–4
[23] Lv T, Ma W, Xin G, Wang R, Xu J, Liu D, Liu F and Pan D 2012 *J. Hazard. Mater.* **237**–**238** 121–32
[24] Prikhod'ko R V, Sychev M V, Astrelin I M, Erdmann K, Mangel A and van Santen R A 2001 *Russ. J. Appl. Chem.* **74** 1621–6
[25] Li F, Jiang X, Evans D G and Duan X 2005 *J. Porous Mater.* **12** 55–63
[26] Langford J I and Wilson A J C 1978 *J. Appl. Crystallogr.* **11** 102–13
[27] Kloprogge J T, Hickey L and Frost R L 2004 *J. Solid State Chem.* **177** 4047
[28] Kloprogge J T, Hickey L and Frost R L 2005 *Mater. Chem. Phys.* **89** 99–109
[29] Kloprogge J T, Hickey L and Frost R L 2004 *J. Raman Spectrosc.* **35** 967–74
[30] Kagunya W, Baddour-Hadjean R, Kooli F and Jones W 1998 *Chem. Phys.* **236** 225–34